UNIVERSITY OF CALIFORNIA, SAN DIEGO

Hydrogen/Deuterium-exchange (DXMS) Analysis of the PKG Iβ Regulatory Domain

A Thesis submitted in partial satisfaction of the requirements for the degree
Master of Science

in

Biology

by

Jun Ho Lee

Committee in charge:

Professor Virgil L. Woods Jr., Chair
Professor Russell Doolittle, Co-Chair
Professor Steven Wasserman
Professor Darren Casteel

2010

The Thesis of Jun Ho Lee is approved and it is acceptable in quality and form for publication on microfilm and electronically:

_____

_____
Co-Chair

_____
Chair

University of California, San Diego

2010

DEDICATION

Foremost I want to dedicate this to my wonderful family. Thank you all for your love and continual support.

To my father, Gi Jung, who taught me the importance of hard work and life-long learning.

To my mother, Fabiola, who instilled in me the desire to become the best I can be.

To my sister, Mariana, for filling my life with joy

TABLE OF CONTENTS

LIST OF FIGURES

LIST OF SUPPLEMENTAL TABLES

ACKNOWLEDGMENTS

I would like to thank Dr. Virgil L. Woods, Jr. for all his support and guidance as my advisor and as the committee chair. I am truly grateful for having the opportunity to work with someone whose passion for his work also instills enthusiasm to everyone else around him.

I would also like to thank Dr. Darren Casteel for all his support. Certainly, this thesis would not have been possible without him. He has served as a great mentor and I am thankful for all his teachings and advice.

I would also like to thank Dr. Russell Doolittle and Dr. Steven Wasserman for being members of my committee. Thank you for providing frequent feedback throughout this project.

Last but not least, I'd like to thank all the members of Woods lab, especially Simon Hsu, Sheng Li, and Tong Liu for their guidance and moral support. Thank you all for providing frequent feedback throughout this project.

The Materials and Methods section, in part is currently being prepared for submission for publication of the material with coauthors Sheng Li, Choel Kim, Virgil L. Woods, and Darren E. Casteel. The thesis author was the primary investigator and author of this material.

The Results section, in part is currently being prepared for submission for publication of the material with coauthors Sheng Li, Choel Kim, Virgil L. Woods, and Darren E. Casteel. The thesis author was the primary investigator and author of this material.

The discussion section, in part is currently being prepared for submission for publication of the material with coauthors Sheng Li, Choel Kim, Virgil L. Woods, and Darren E. Casteel. The thesis author was the primary investigator and author of this material.

ABSTRACT OF THE THESIS

Hydrogen/Deuterium-exchange (DXMS) Analysis of the PKG Iβ Regulatory Domain

by

Jun Ho Lee

Master of Science in Biology

University of California, San Diego, 2010

Professor Virgil L. Woods Jr., Chair

Professor Russell Doolittle, Co-Chair

The type I cGMP-dependent protein kinases play critical roles in regulating vascular tone, platelet activation and synaptic plasticity. PKG I α and PKG Iβ differ in their first ~100 amino acids giving each isoform unique dimerization and autoinhibitory domains with identical cGMP-binding pockets and catalytic domains. The N-terminal leucine zipper and autoinhibitory domains have been shown to mediate isoform specific affinity for cGMP. PKG Iα has a >10 fold higher affinity for cGMP than PKG Iβ, and PKG Iβ missing its leucine zipper has a three-fold decreased affinity for cGMP. The exact mechanism through which the N-terminus of PKG alters cGMP-affinity is unknown. In the present study, we have used deuterium exchange mass spectrometry to study how PKG Iβ's N-terminus affects the conformation and dynamics of its cGMP-binding pockets. We found that the N-terminus increases the rate of deuterium exchange

throughout the cGMP-binding domain. Our results suggest that the N-terminus shifts the conformational dynamics of the binding pockets, leading to an ‘open’ conformation that has an increased affinity for cGMP.

Introduction

1.1 Hydrogen/Deuterium Mass Spectrometry

Understanding the folding and conformational changes a protein undergoes is essential in the design of small molecule drugs that target specific enzymes. In the last few decades, advancements in X-ray crystallography and high-resolution NMR have yielded a very large number of extremely valuable protein structures; however, information on protein dynamics lagged behind because of a lack of robust methods and analytical tools[1]. Peptide amide hydrogen exchange is an approach to study the thermodynamics of protein conformational changes and the mechanism of protein folding [2,3]. Both structure and dynamics contribute significantly to the function of proteins, and therefore, to fully understand a protein, the interplay of structure, function, and dynamics must be investigated[4].

Hydrogen exchange coupled to mass spectrometry (DXMS) has become a valuable analytical tool for the study of protein dynamics and changes to protein conformation[5]. Traditionally, hydrogen exchange methodology has been used in conjunction with NMR analysis, but recent advances in mass spectrometry technology have made mass spectrometry the preferred choice for the systematic study of proteins[6]. Recent developments in the field offer better spatial resolution, automation of the labeling and automation of the data processing, and the ability to analyze larger complex proteins with ever smaller amounts of material[4]. Hydrogen exchange coupled with mass spectrometry has thus become a powerful tool in the study of protein dynamics. In this study, DXMS will be used to study the structural dynamics of Type Iβ cyclic GMP-dependent protein kinase (PKG Iβ)

1.2 Theory of Hydrogen Exchange

Hydrogen exchange studies exploit the fact that the acidic hydrogens on a protein are not permanently attached, but are continually exchanging with solvent protons. These exchanging hydrogens include -OH, -NH, and -SH side chain moieties, and the amide hydrogen of the peptide bond, excluding that of proline[7]. Only peptide amide hydrogens exchange slowly enough to be experimentally accessible in most methodologies and their rate of exchange is dependent on the peptide bond accessibility to solvent[8].

In a folded protein, backbone amide hydrogen exchange rates are highly variable and can range over eight orders of magnitude[1]. The variation of exchange rates reflect the diversity of local environments for individual amide hydrogens such as solvent accessibility, hydrogen bonding, and local inductive effects caused by adjacent amino acids[9]. Amide hydrogens must make physical contact with the surrounding solvent for exchange to occur[10]. For amide hydrogens in structured regions, fluctuations must occur that break local hydrogen bonds, disrupt local structure and transiently expose the NH's to solvent[8]. However, stability is not distributed uniformly throughout protein structure, with less stable regions undergoing more frequent local unfolding, leading to increased hydrogen exchange. Solvent exposed amide hydrogens, such as those found in unstructured regions, will readily exchange protons with water while hydrogens that are either buried within the protein or are involved in hydrogen bonding reactions will exchange at a slower rate [11]. Thus, hydrogen exchange rates provide information on the conformational properties of a folded protein.

1.3 Hydrogen/ Deuterium Exchange with Mass Spectrometry (DXMS)

Hydrogen exchange rates can be measured by incubating the protein in D_2O and

then tracking deuterium incorporation in various parts of the protein through mass spectrometry. DXMS experiments are performed as follows (Fig. 1). An initial *functional labeling step*, is performed under entirely physiologic conditions of pH, ionic strength, and buffer salts, and is followed by a subsequent localization step, performed under non-physiologic conditions. When measuring *on-exchange*, the protein is incubated in deuterated water; aliquots are taken over an appropriate period of time, usually 10 to 3000 sec, and each aliquot is "quenched" to retard further deuterium exchange by quickly acidifying (to pH ~2.5) and cooling the sample. The quench buffer contains a 0.8% formic acid, which quickly lowers the pH and greatly slows the exchange reaction. The quench buffer also contains guanidium hydrochloride to denature the protein. Protein denaturation accomplishes two goals; i) it aids in halting the exchange reaction at sites of low accessibility and ii) the denatured protein is more accessible to the pepsin protease during its exposure to the pepsin column. Undesired "back-exchange", or loss of label, is minimized by performing all subsequent manipulations under quench conditions, and by holding samples at -80ºC. In the *localization step*, the protein is extensively proteolyzed into overlapping fragments of 5-20 amino acids and subjected to LC/MS. Peptides that contain deuterium are identified and their deuterium content quantified. By plotting the deuterium content of the peptides as a function of time, one can infer exchange rates for amide hydrogens in each region of the protein.

1.4 cGMP-dependent protein kinase

The cGMP-dependent protein kinases (PKGs) are involved in a variety of cellular processes including regulation of vascular tone, platelet activation, and synaptic transmission[12, 13]. Mammalian cells express three different PKGs from two separate

genes. There are two type I PKGs (PKG Iα and PKG Iβ) and one type II (PKG II). Each family member has an N-terminal regulatory domain and a C-terminal catalytic domain, with the regulatory domain containing conserved sub-domains including a leucine zipper, followed by an autoinhibitory loop and two tandem cGMP-binding pockets[13] as shown in Figure 2. At the extreme N-terminus, a leucine zipper domain mediates homo-dimerization and targets the kinase to isoform-specific interacting proteins[15, 16, 21]. The leucine zipper is followed by an autoinhibitory domain, which contains autophosphorylation sites and a pseudo-substrate sequence that inhibits kinase activity by binding within the substrate recognition cleft of the catalytic domain in the absence of cGMP[27]. Next, two-tandem cGMP-binding pockets mediate kinase activation in response to increased cellular cGMP levels. The more N-terminal binding pocket (domain A) has a higher affinity for cGMP than the C-terminal pocket (domain B); this order is the reverse from what is seen for the cyclic nucleotide binding pockets in PKA[32]. The cGMP-binding pockets are followed by the catalytic domain which can be divided into a small lobe that binds Mg2+ATP and a large lobe that mediates substrate recognition[33].

PKG Iα and PKG Iβ are splice variants which have identical catalytic and regulatory domains but differ in their first ~100 amino acids, which contain isoform specific leucine zippers and autoinhibitory domains[13]. The leucine zippers of PKG Iα and PKG Iβ have at least three functions. They mediate isoform-specific homodimer formation, they mediate specific protein-protein interactions and they are at least partly responsible for isoform-specific cGMP affinity[14-21]. While the molecular details of dimer formation and protein-protein interactions have been reported [15, 16], at this time it is unclear how the N-terminus affects cGMP-binding to the kinases. PKG Iα and Iβ differ

only in their N-terminal dimerization and autoinhibitory regions, and even though they have identical amino acid sequences in their cyclic nucleotide binding pockets, they differ 5- to 10-fold in their affinity for cGMP [23,24]. Studies by Ruth *et. al.* demonstrated that isoform-specific kinase activation constants (*Ka*) could be localized to specific amino acid sequences in the leucine zipper and autoinhibitory domains[14]. Later, Richie-Jannetta *et. al.* found that isolated PKG Iα and PKG Iβ regulatory domains (i.e. PKG lacking the catalytic domain) retained isoform-specific cGMP-binding properties and underwent distinct conformational changes, as determined by Stokes radius [23]. Other studies have shown that PKG Iβ lacking its N-terminal leucine zipper domain has a two-three fold lower affinity for cGMP [25]. From these studies it is clear that the isoform-specific affinities for cGMP reside entirely within the regulatory domains, and that the leucine zipper and/or autoinhibitory domain(s) somehow affect the conformation of the cGMP-binding pockets. Yet how the N-terminal 100 amino acids of PKG Iα and PKG Iβ affect the cGMP-binding pockets is unknown.

Deuterium exchange mass spectrometry (DXMS) is an ideal method for probing the structural/conformational dynamics of proteins[26]. The technique uses mass spectrographic analysis to measure time dependent deuterium incorporation into the amide hydrogens of the peptide backbone. Since exchange rates are determined by solvent accessibility and the stability of secondary structure hydrogen bonds, DXMS provides a sensitive way to measure changes in protein structure and dynamics in response to ligand binding, protein-protein interactions, and interdomain interactions. Previous deuterium exchange experiments on full-length PKG Iα have demonstrated that cGMP binding leads to increased deuterium incorporation into residues within the

autoinhibitory loop and catalytic cleft of the kinase and supported a model of PKG activation in which, in the absence of cGMP, the autoinhibitory loop binds within the catalytic cleft and maintains the kinase in an inactive state[27]. cGMP binding is thought to induce a conformational change in the regulatory domain that releases the autoinhibitory loop from the catalytic cleft, allowing access to substrates. How the N-terminus of PKG affects cGMP affinity was not addressed.

In the results presented here, we used deuterium exchange mass spectrometry to study how the N-terminus of PKG Iβ affects the conformational dynamics of PKG Iβ's cGMP-binding pockets. Proteins consisting of the full-length regulatory domain (residues 4-352) or just the two cGMP-binding pockets (residues 98-352) were examined. We found that in the presence of the N-terminus, the rate of H/D exchange is increased throughout the cGMP-binding pockets, indicating an increased dynamic state. We infer that increased dynamic state causes the binding pockets to adopt a more 'open' state, allowing access for cGMP.

Methods and Materials

2.1 DNA Constructs

N-terminal fragments of PKG Iβ consisting of residues 4-352 and 98-352 were created using polymerase chain reaction and the following primers: 5' GATGGATCCTTG-CGGGATTTACAGTAC-3' (4-352 forward); 5'-GATGGATCCTTCTACCCCAAGAGCCCAC -3' (98-352 forward); 5'-GATGAATTCTTATTATTCATATGCTTTATT-AGAAAC-3' (common reverse). The PCR products were digested with *BamHI/EcoRI* and ligated into *BamHI/EcoRI* digested pRSET-Xa. Vector pRSET-Xa was created by digesting pRSET B (Invitrogen) with NheI/HindIII and ligating a linker composed of the primers: 5'-CTAGCATTGAGGGACGCGGATCCGCACTCGAGGCAGAAT-TCGA-3' (sense) and 5'-AGCTTCGAATTCTGCCTCGAGTGCGGATCCGCGTCCCTCAATG-3' (antisense). In mammalian cells, PKG Iβ is processed and lacks an N-terminal methionine, and begins with the amino acid sequence GTLRDL-. Since the extreme N-terminus of PKG Iβ has no effect of cGMP affinity and to facilitate the introduction of a *BamHI* fusion site, our construct begins GSLRDL, with the *BamHI* site coding for the GS residues and the fourth amino acid (L) being the first conserved amino acid within our construct. All vectors were sequenced to insure the absence of PCR induced mutations.

2.2 Protein Purification

Recombinant proteins were expressed in BL21 *E. coli* at 30ºC using LB Media. Bacteria were harvested by centrifugation, resuspended in ice cold 50 mM potassium phosphate and 500 mM NaCl (pH 8.0) and lysed by sonication. The lysate was cleared by centrifugation and recombinant proteins were purified by nickel affinity

chromatography using Profinia resin (BioRad). Eluted proteins were concentrated to 2 ml and further purified over a sepharose 200 HR column equilibrated in buffer B (20 mM Tris, 150 mM NaCl and 5% Glycerol). Fractions containing the recombinant proteins were pooled and concentrated to 5-10 mg/ml. Protein concentrations were determined by A_{280}. All post lysis purification steps were performed at 4ºC. Proteins were stored on ice until DXMS analysis (less than 24 hours).

2.3 Peptide Fragment Optimization

The optimum buffer conditions for DXMS analysis were determined by performing test digests of 50 μg recombinant protein with 0.5, 1.0 and 2.0 M guanidium-hydrochloride quench buffers (all quench buffers contained 0.8% formic acid and 16.6 % glycerol). Specifically, 60 μl buffered water (which mimics the deuterium used for exchange reactions) was added to 100 μg recombinant protein in a total volume of 20 μl (all manipulations were done on ice). Then, 120 μl ice cold quench buffer was added and the sample was split into two 100 μl aliquots. The samples were frozen on dry ice and stored at -80ºC until analysis by mass spectrometry.

2.4 Deuterium on Exchange

All deuterium exchange reactions were performed on ice in a cold room at 4ºC. Exchange reactions were initiated by adding 60 μl buffered D_2O to 20 μl purified PKG. At the appropriate time point exchange was quenched by adding 120 μl 1.6M GuHCl/0.8% Formic Acid. The samples were split into two 100 μl aliquots and frozen on dry ice. Frozen samples were stored at -80ºC until analysis by mass spectrometry. To analyze deuterium exchange profiles in the presence of cGMP, aliquots of purified PKG

Iβ peptides were incubated with 1 mM cGMP on ice for 3 h before performing exchange reactions.

2.5 Data Acquisition and Analysis

Samples were analyzed through an automatic apparatus that thawed and proteolyzed frozen samples, which was followed by LC-MS analysis of the resulting peptide. The samples were passed through an immobilized pepsin column and the protease-generated fragments were collected on a C18 HPLC column. The effluent was then directed to a Thermo Finnigan LCQ electrospray ion trap type mass spectrometer with data acquisition in either MS1 profile mode or data-dependent MS2 mode. The pepsin-generated peptides from the MS/MS data sets were identified using SEQUEST (Thermo Finnigan Inc.). This set of peptides was then further analyzed using specialized DXMS data reduction software (Sierra Analytics Inc., Modesto, CA). Corrections for back exchange were made through measurement of loss of deuterium from reference protein samples that had been equilibrium-exchange-deuterated under denaturing conditions. Deuterium incorporation was thus calculated via the methods of Zhang and Smith:

$$\text{deuteration level } (\%) = \frac{m(P) - m(N)}{m(F) - m(N)} \times 100$$

Where $m(P)$, $m(N)$, and $m(F)$ are the centroid value of the partially deuterated, nondeuterated, and fully deuterated peptide, respectively[31]. The experiments were performed twice using independent protein preparations, and the reported results are the average of the two experiments.

2.6 Model Building

A PKG Iβ molecular model was built using the automated Swiss Model homology-modeling server at the Swiss Institute of Bioinformatics (University of Basel, Switzerland) (66). The model was constructed using a cAMP-bound PKA structure (PDB 1RGS) as a template. Specifically, cGMP-binding pockets were modeled by threading the PKG Iβ sequence into solved structures for cAMP-dependent protein kinase. Sequence alignments were performed using clustalW, with minor manual adjustments.

2.7 Acknowledgement

This section, in part is currently being prepared for submission for publication of the material with coauthors Sheng Li, Choel Kim, Virgil L. Woods, and Darren E. Casteel. The thesis author was the primary investigator and author of this material.

Results

3.1 PKG Iβ Domain Organization and Regulatory Domain Constructs Used for DXMS Analysis

Full-length PKG cannot be functionally expressed in *E.coli*, presumably due to the lack of activation loop phosphorylation and misfolding of the catalytic subunit[34]. Even though it lacks kinase activity, the soluble fraction of full-length PKG Iα expressed in *E.coli* still binds cGMP with high affinity, indicating that functional regulatory domains can be expressed in *E.coli*; this finding has been supported by others[35]. Previous studies have shown that the isolated regulatory domains of PKG Iα and PKG Iβ retain cGMP-binding characteristics of the full-length proteins[23]. Therefore, to produce proteins for DXMS analysis, full-length and truncated versions of the PKG Iβ regulatory domain (residues 4-352 and 98-352, respectively, see Fig. 2) were expressed in *E.coli* and purified as described in Materials and Methods.

3.2 Tuning of PKG Iβ 4-352 and PKG Iβ 98-352 Proteolytic Fragmentation

We began our analysis of the mechanism by which the PKG Iβ N-terminus affects cGMP-affinity of the binding pockets by determining the conditions that produced the optimal number of peptides during proteolysis over a pepsin column. To accomplish this we tested various concentrations of Guanidium in the quench buffer (0.5, 1.0 and 2.0 M) and found that a final concentration of 1 M was optimal. Under these conditions we obtained 117 peptides for PKG Iβ 4-352 and 196 peptides for PKG Iβ 98-352. Within the cGMP-binding pockets, there were 71 peptides in common between the two proteins; these are shown in Figure 3. Unfortunately, peptides within the leucine zipper region of

PKG 4-352 were not identified. Interestingly, when a protein comprising the PKG Iβ leucine zipper (residues 4-55) was subjected to DXMS analysis we found that the leucine zipper domain was not proteolyzed under the conditions typically used in DXMS, highlighting the tightly folded and stable nature of this domain (data not shown).

3.3 Deuterium on Exchange of PKG Iβ 4- 352

PKG I β 4-352 (+/- cGMP) was incubated in deuterated buffer, on ice, for various time points and quenched with 1.5 volumes 1.6 M GuHCl/0.8% formic acid to minimize the exchange reaction and prevent back-exchange. The amount of deuterium incorporation was determined by mass spectrometry, and percent deuterium incorporation was determined as described in Materials and Methods (see Supplemental tables 1 and 2). A color bar representation showing percentage deuteration of selected peptides is shown in Figure 4. Predicted secondary structural elements, based on alignment to PKA RIα, are shown above the sequence. As described above, peptides within the leucine zipper domain could not be detected. We found that residues 71-86, in the autoinhibitory loop, were fully deuterated at the shortest time point examined (3 seconds), even in the absence of cGMP, and showed no change in deuterium incorporation in the presence of cGMP. As expected, our results differ from those previously seen with full-length PKG Iα[27]. In full-length PKG Iα, in the absence of cGMP, the autoinhibitory loop is protected from H/D exchange, and this protection is most likely the result of the autoinhibitory loop binding within the substrate binding cleft of the catalytic subunit. Therefore, our data is consistent with the predicted model for PKG regulation in which the autoinhibitory loop,

in full-length PKG I, is bound to and inhibits the catalytic domain in the absence of cGMP.

In the presence of cGMP, deuterium incorporation was reduced throughout the rest of the protein (residues 89-352) with regions at the C-terminus of each binding pocket being most affected (residues 172-210 and 304-331). These residues span β5-β8 in domain A and β6-β8 in domain B; they include the P-helices that lie between β6 and β7 in each pocket and encompass the phosphate binding cassettes (PBCs), which coordinate binding of the cyclic nucleotide phosphates within each binding pocket. In crystal structures of cAMP-bound PKA RIα and RIIβ, the amide hydrogens in this region are involved in multiple hydrogen bonding events that are stabilized by nucleotide binding. These hydrogen bonds include those that form the short P-helix[36, 37.] We also observed that peptides at the extreme C-terminus of this construct (residues 346-352) have decreased deuterium incorporation in the presence of cGMP; these residues are predicted to form the C-helix at the end of domain B, which in PKA splits into two separate helices upon binding to the C-subunit[38]. Our data suggests that this region contributes to the cGMP-induced conformational changes that activate PKG.

3.4 Deuterium on Exchange PKG Iβ 98- 352

PKG Iβ 98-352 (+/-) cGMP was subjected to H/D exchange and mass spectrographic analysis as described above for PKG Iβ 4-352 (see Supplemental tables 3 and 4). As expected, and like PKG Iβ 4-352, deuterium incorporation into the nucleotide binding pockets was reduced in the presence of cGMP. Interestingly, when deuterium incorporation into PKG Iβ 98-352 was compared to deuterium incorporation obtained for

PKG Iβ 4-352, an overall decrease in deuterium incorporation in peptides throughout the cyclic nucleotide pockets was evident, with certain peptides being more affected than others. Differences in exchange behavior between identical peptides from cGMP PKG Iβ 4-352 and PKG 98-352, in the absence of cGMP, at three different time points, are shown in Figure 5. At the shortest time point examined, there are four regions that are specifically affected. These regions span amino acids 114-124, 219-230, 307-314 and 346-352. Based on homology to PKA, residues 114-124 are predicted to form part of the N- and 3_{10}-helicies that are part of an N-3-A motif, which undergoes major conformational changes during kinase activation[39]. Residues 219-230 are within the C-Helix that connects the two cyclic nucleotide binding pockets and residues 346-352 are predicted to be part of the C-helix in domain B; these regions are also predicted to undergo major conformational shifts during kinase activation. Finally, residues 307-314 make up the P-helix in the second cGMP-binding pocket, which is stabilized by cGMP-binding; how the increased H/D exchange rate of these P-helix residues contributes to increased cGMP affinity is not readily evident. It is interesting that most of the regions that show the greatest increase in H/D exchange, in the presence of the N-terminus, are located in helical regions, which in analogy to PKA are predicted to undergo dramatic conformational changes during kinase activation. This suggests that the N-terminus may increase cGMP affinity by positioning these helices in a conformation that mimics the active, cGMP-bound, conformation (discussed below). While PKA structures have shown dramatic changes in the relative conformation of the helical domains as the R-subunits shift from cAMP to C-subunit bound forms, the conformation of the β-strands barely change[36-38, 40]. Along these lines, the area with the least difference in H/D

exchange in the absence of the N-terminus appears to be within the β-strands, with β7 and β8 in domain A being the least affected. At later time points, the differences in H/D exchange are localized to different areas within the cGMP-binding pockets, partially due to saturation of fast exchanging sites, but the general trend of an overall decrease in H/D exchange in the absence of the N-terminus remains constant.

3.5 Modeled cGMP Binding Pockets

In order to thoroughly interpret our DXMS data, we wanted to examine it based on three dimensional structures. There are no crystal structures of PKG Iβ's cGMP-binding pockets, but there exist multiple structures of PKA, so we built models of PKG Iβ using the PKA RIα structure as a template; this model is shown in Figure 6. As can be seen, the regions that become most protected upon cGMP binding (residues 173-184 in the A-domain and residues 305-314 in the B-domain) are located in the PBCs at the base of the cGMP-binding pocket. The peptide consisting of residues 217-227, which lies within the C-helix and connects the two cNBDs, has a dramatically different H/D exchange profile in the presence and absence of cGMP. One salient difference is that PKG containing the N-terminus the C-helix responds to cGMP binding whereas in the 98-352 construct the response is severely attenuated. Interestingly, DXMS analysis of PKA RIα and RIIβ demonstrated isoform specific differences in H/D exchange; cAMP-binding led to decreased exchange in RIα but had no effect on RIIβ. Our results show that in the presence of the N-terminus, residues within the C-helix have a very pronounced cGMP-dependent decrease in H/D exchange which suggests that it undergoes conformational changes that mirror those in RIα and not RIIβ.

3.6 Acknowledgement

This section, in part is currently being prepared for submission for publication of the material with coauthors Sheng Li, Choel Kim, Virgil L. Woods, and Darren E. Casteel. The thesis author was the primary investigator and author of this material.

Discussion

We have used DXMS to study how the N-terminus of PKG Iβ modulates cGMP affinity of the nucleotide binding pockets. In experiments examining PKG Iβ 4-352, we found that the autoinhibitory domain has an extremely fast exchange rate that was not altered by cGMP binding; indicating that this region is unstructured, and as such probably not involved in modulating cGMP-affinity within the isolated regulatory domains. Thus, cGMP-affinity is most likely modulated by the leucine zipper domain alone. In fact, residues within the leucine zipper have been shown to modulate the isoform specific *Ka* values in full-length PKG Iα and PKG Iβ[14], but these studies also demonstrated that residues within the autoinhibitory region were also involved in modulating isoform specific *Ka* values. This discrepancy can be reconciled by analogy to studies on PKA which suggest that cGMP-binding and PKG activation may not be completely correlated. Small angle X-ray scattering experiments on PKA have shown that RIα:C-subunit and RIIβ:C-subunit complexes persist even in the presence of saturating concentrations of cAMP[41]. While addition of a substrate peptide causes complete disassociation of the RIα:C-subunit complex, the RIIβ:C-subunit complex is partially retained[41]. In PKG, the regulatory and catalytic subunits reside on the same peptide chain, therefore this phenomenon, in which the cyclic-nucleotide bound regulatory domain continues to bind and inhibit the catalytic domain, may be even more prevalent. Another complicating factor in relating *Ka* values to cGMP-binding affinity is the fact that both PKG Iα and PKG Iβ are activated by autophosphorylation within their autoinhibitory domains[42]. Thus in the full-length kinases, the role of the autoinhibitory regions in altering isoform

specific kinase activation may be due to their different levels of autophosphorylation, rather than in their ability to modulate cGMP-affinity.

Comparing cGMP-bound and unbound PKG Iβ, we found that deuterium incorporation is reduced throughout the cGMP-binding pockets, with regions most affected being residues within and flanking the phosphate binding cassette. This result is similar to what was found in DXMS analysis of PKA [43,44] and can be explained by the stabilization of inherent secondary structure elements in the cNBD and the large number of hydrogen bonds that form between the cyclic nucleotide's phosphate and the protein's main chain amide groups [36,37]. Thus, our results strongly suggest that the molecular interactions involved in binding the cyclic nucleotide phosphate in PKA, especially the stabilization of the B'-helix, are conserved in PKG.

We found that the N-terminus of PKG I caused an increased rate of deuterium incorporation throughout the cGMP-binding domain. This result was unexpected, in that we anticipated that the N-terminus would increase cGMP affinity by stabilizing the folded state of the binding pockets. Based on our results we now propose that the N-terminus increases cGMP-affinity within the binding pockets by inducing a conformational change that produces an 'open' conformation allowing cGMP access. The basis of this open conformation can be understood in the context of protein dynamics in which proteins exist in multiple conformational states and ligand binding simply stabilizes a preexisting conformation [45, 46]. Based on this model we predict that the increased dynamics induced by the N-terminus of PKG I causes the cGMP-binding pockets to spend relatively more time in a conformation that mirrors the cGMP-bound form, thereby increasing cGMP-affinity.

We expected to identify the residues where the N-terminus contacts the cGMP-pockets, which would have appeared as a region within the binding pockets that had decreased deuterium incorporation in the presence of the leucine zipper. We were unable to identify such a region, and the reason for this may be due to the very dynamic and unstructured nature of the autoinhibitory loop that connects the leucine zipper to the cNBDs; thus the interaction between the binding pockets and the leucine zipper may be very dynamic and undetectable using our experimental protocol. In fact, while there are many solved structures for the various isoforms of PKA regulatory subunits, encompassing either the cAMP-binding pockets [36-38, 40]or the N-terminal dimerization/docking domain [47-49], as yet there are no structures for a full-length PKA regulatory domain. It has been proposed that the autoinhibitory loop between the two domains is very dynamic and thus complexes containing the two domains may be very difficult to crystallize [50]. Likewise, our inability to detect an interaction interface between PKG I's N-terminus and the cGMP-binding pockets, suggest that it may be difficult to obtain crystal structures of full-length PKG. While structures of PKGs nucleotide binding pockets, in both cGMP-bound and unbound forms, would be extremely valuable for designing isoform specific PKG activators and inhibitors, the fact that the N-terminus affects the conformation and/or dynamics of the binding pockets means that crystal structures will not provide isoform-specific information.

The residues that have the largest increase in H/D exchange rates in the presence of the N-terminus are within the C-helix, which connects the two binding pockets. In PKA, the B- and C-helicies undergo a dramatic conformational change between C-subunit bound and unbound states [38]. In fact, when bound to the C-subunit the B and C

helices form one long B/C helix[38]. Since the B/C helix connects the two cNBDs its conformation likely plays a role in controlling communication between the two binding pockets. In PKA, the B/C helix also makes direct contact with the C-subunit, and plays a critical role in mediating kinase inhibition[38]. DXMS analysis of PKA RIα and RIIβ revealed that residues within the B/C helix underwent isoform specific responses in response to cAMP binding[43, 44]. In RI residues 232-247 showed a decreased rate of H/D exchange in the presence of cAMP, an analogous peptide in RII showed no change. Interestingly, a peptide within the C-helix of PKG I (residues 217-227) showed a cGMP-induced decrease in H/D exchange in the presence of N-terminus, and this decrease was markedly reduced when the N-terminus was absent. This result suggests that cGMP-induced conformational changes within the C-helix of PKG I may be similar to those in PKA RI and that PKG I's N-terminus plays a critical role in mediating those changes.

Cyclic nucleotide binding domains in PKG and PKA share an evolutionally conserved set of subdomains, including an N-terminal helical N-3-A motif, an eight stranded β-barrel and a C-terminal helical domain. Data from X-ray crystallography, NMR, and deuterium exchange experiments, comparing the cyclic nucleotide bound and unbound forms of the binding domains, have allowed the elucidation of a general model for cyclic nucleotide induced changes in the binding domains[39]. The cyclic nucleotide binds within the stably folded β-barrel which induces global movements of the N- and C-terminal helical domains, leading to kinase activation. Our data strongly supports a model in which the conformation of PKG Iβ's helical domains is sensitive to the presence of both cGMP and the N-terminus.

In this study we used DXMS to examine the how the N-terminus affects cGMP-affinity within the regulatory domain of PKG Iβ. PKG Iα has its own distinct N-terminus and a higher affinity for cGMP than PKG Iβ, and at this time it is unknown if the N-terminus of PKG Iα has a similar effect on the dynamics of its cGMP-binding pockets. To gain insight into PKG I isoform specific cGMP-affinity, we are currently performing DXMS studies on the isolated regulatory domain of PKG Iα.

Acknowledgement

This section, in part is currently being prepared for submission for publication of the material with coauthors Sheng Li, Choel Kim, Virgil L. Woods, and Darren E. Casteel. The thesis author was the primary investigator and author of this material.

Figures

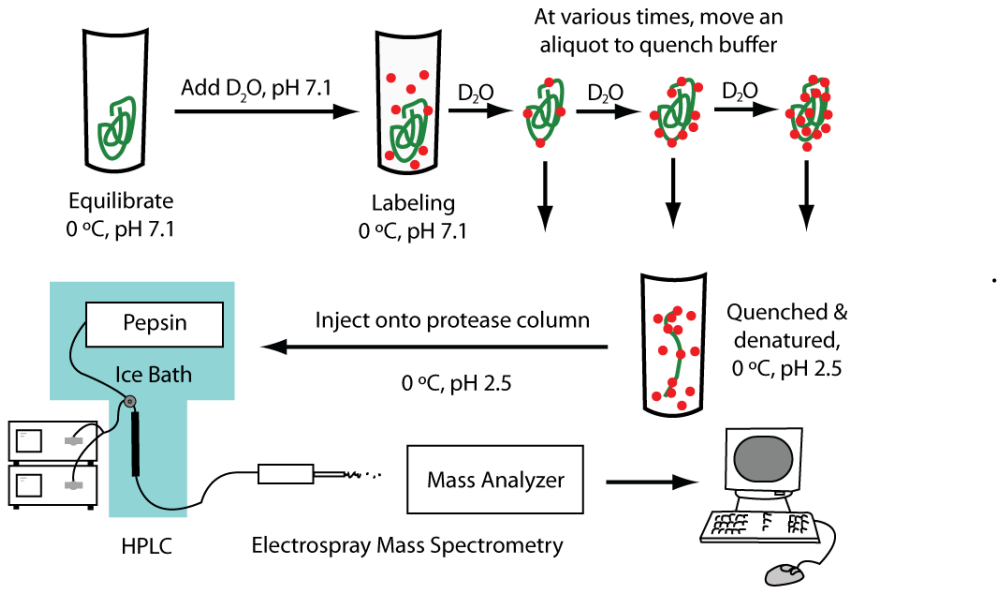

Fig 1: Hydrogen Deuterium Exchange Protocol.
A protein, in its native state, is incubated in D_2O at 0ºC. At various time points, exchange is terminated by lowering the pH, the protein is digested with an acid protease, and peptides are characterized by mass spectrometry. Red dots represent deuterium exchanged onto the protein/peptides.

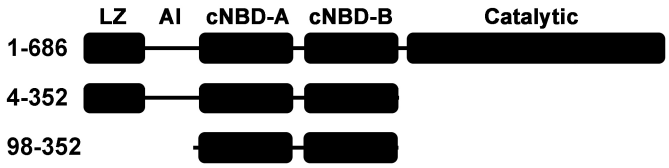

Figure 2: Domain organization of PKG Iβ.
The domain organization of PKG Iβ is shown with constructs used in this study indicated below. PKG Iβ has an N-terminal regulatory domain and a C-terminal catalytic domain. The regulatory domain contains functional sub-domains, including a leucine zipper/dimerization domain (LZ), and autoinhibitory domain (AI) and two tandem cGMP-binding pockets. The catalytic domain is positioned at the C-terminus. The constructs used in this study consists of the complete regulatory domain (residues 4-352) or isolated cGMP-binding pockets (residues 98-352).

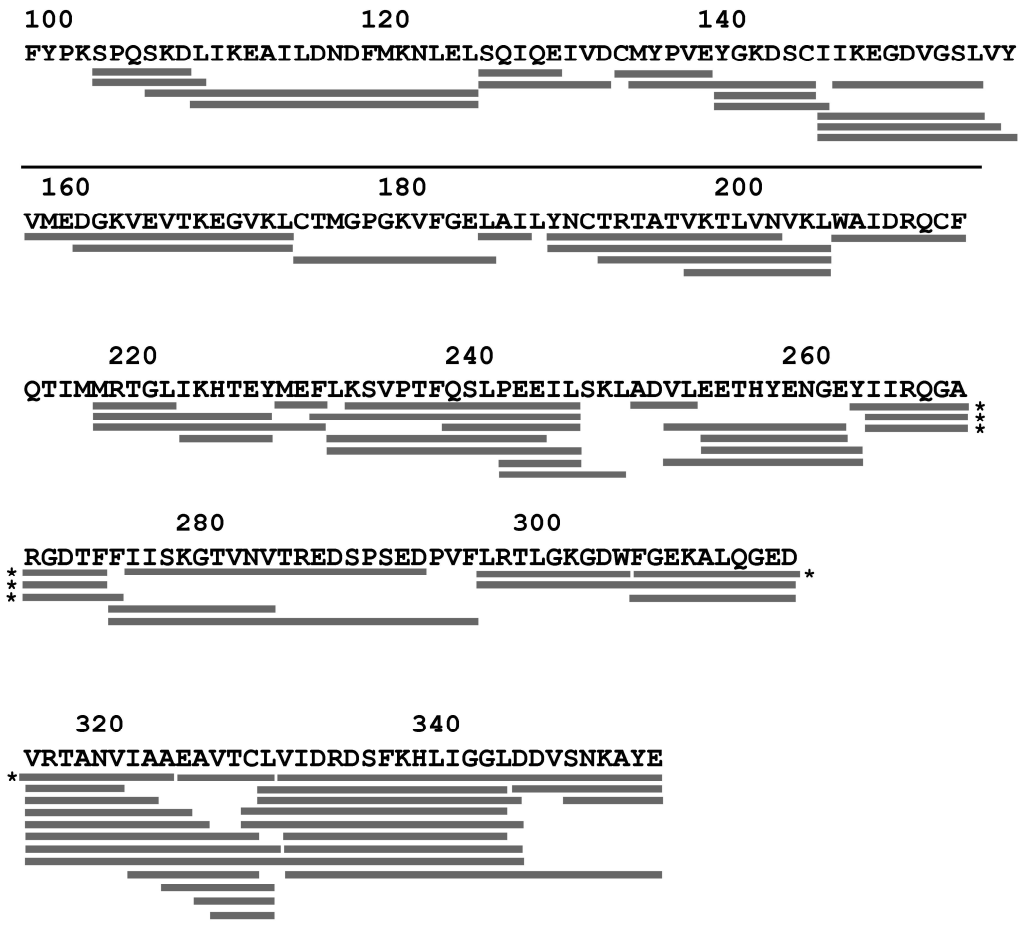

Figure 3: Pepsin digest map of the cGMP-binding region of PKG Iβ
Pepsin digest map showing identified peptides that are in common between PKG Iβ 1-352 and 98-352. The peptides are shown as grey bars below the amino acid sequence.

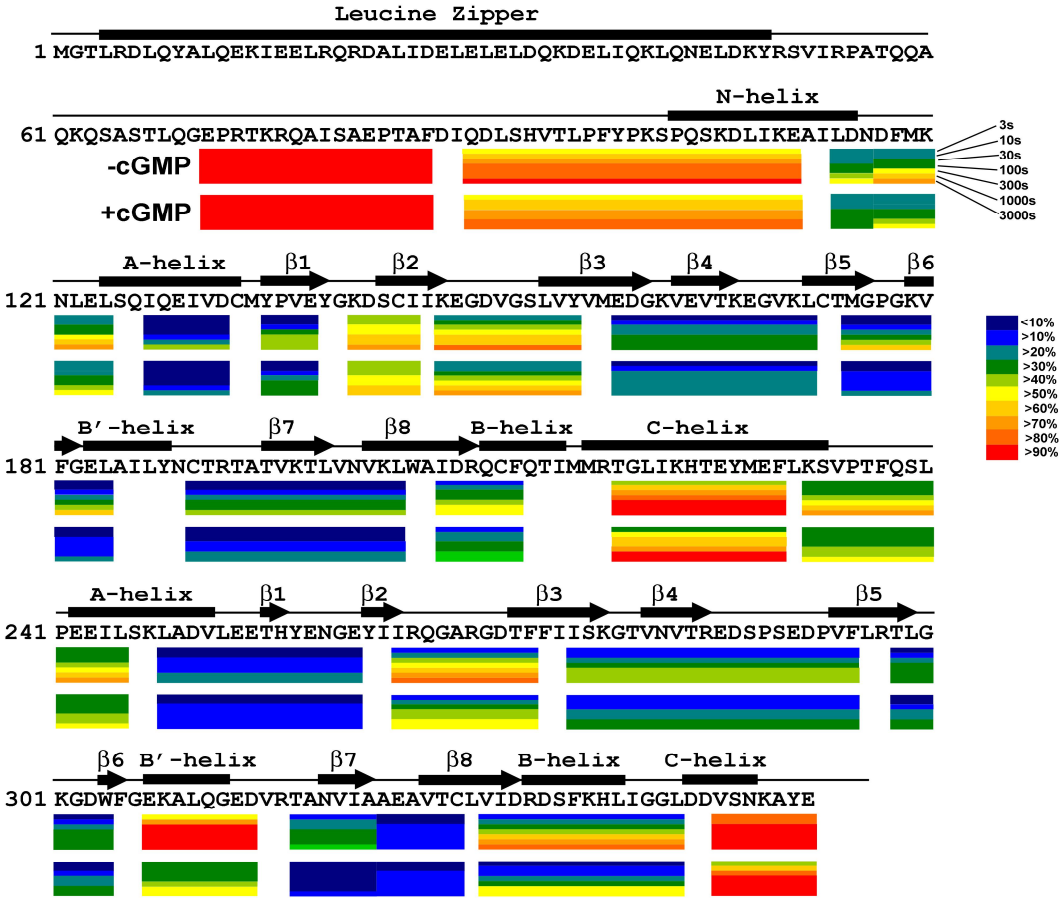

Figure 4: Hydrogen/Deuterium exchange of PKG Iβ 4-352 in the presence and absence of cGMP.

The primary sequence of PKG Iβ is shown with predicted secondary structural elements based on homology to PKA RIα diagramed directly above. Color bars indicating percent deuteration at various time points (3-3000s) are shown below the sequence. Exchange experiments were performed with and without bound cGMP, as indicated. The results are the average of two independent experiments performed on two protein preparations.

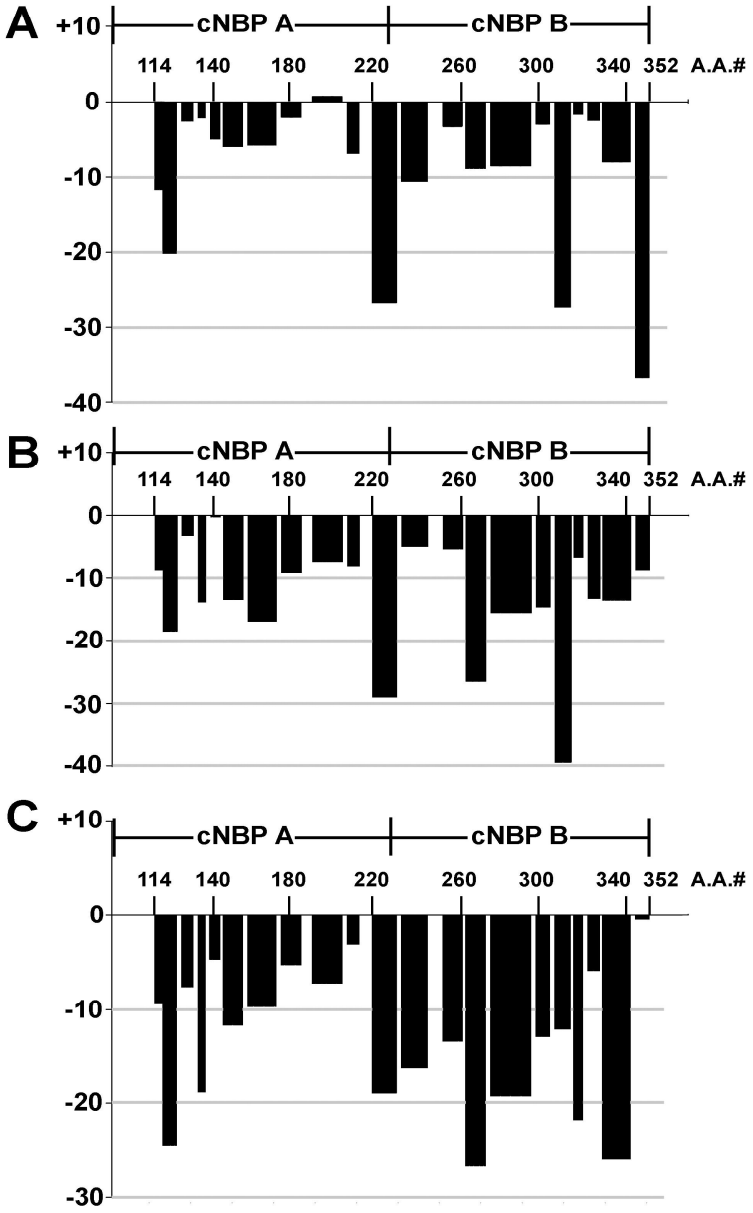

Figure 5: The leucine zipper/autoinhibitory region increases H/D exchange throughout the cGMP-binding domain.
Average difference in deuteration between PKG Iβ 4-352 and PKG Iβ 98-352 at 3, 30, and 300 seconds are shown (labeled A, B and C, respectively.) Negative values represent a decrease in deuteration in the absence of the leucine zipper/autoinhibitory domain.

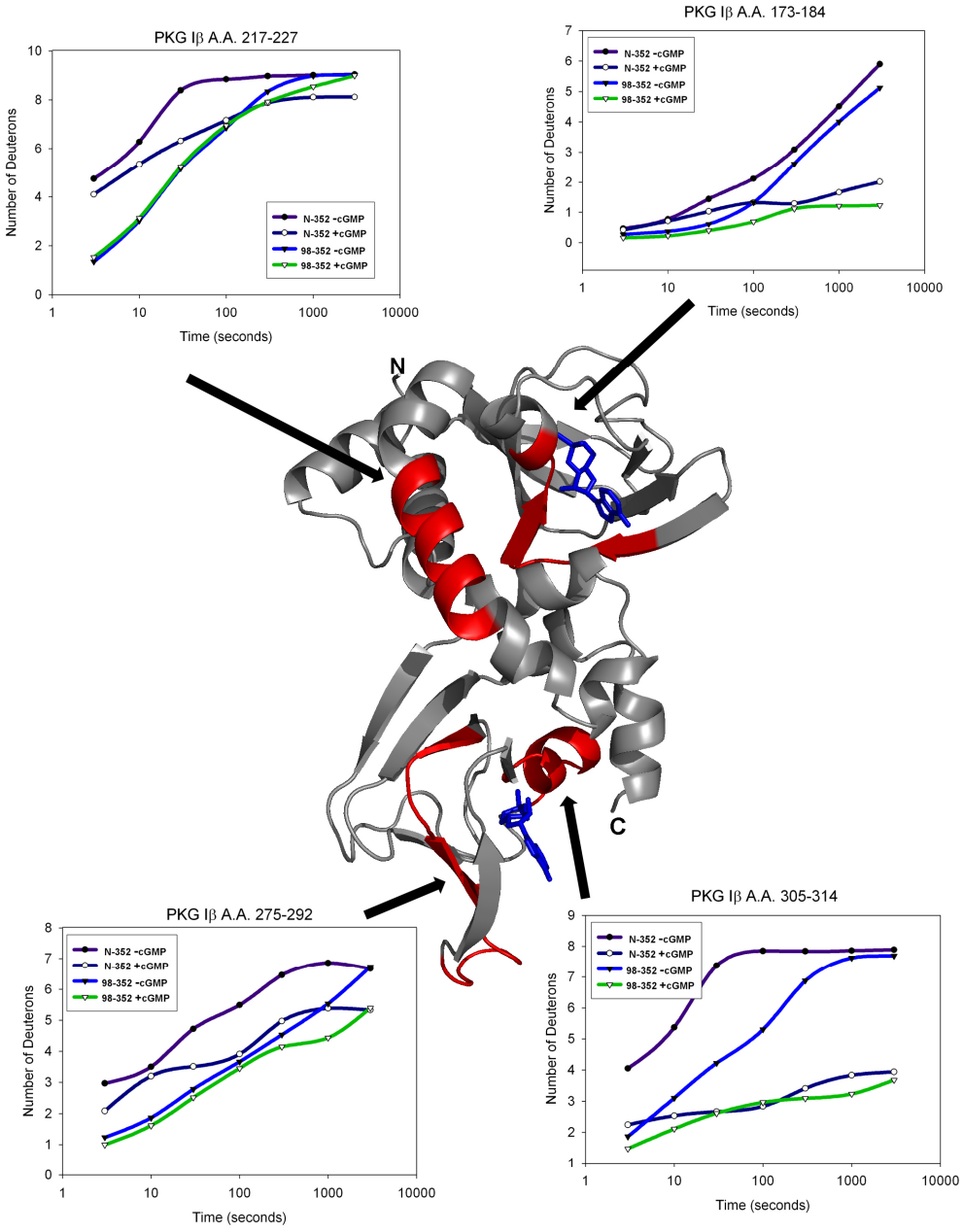

Figure 6. Structural/functional interpretation of the exchange data.
Molecular models of PKG Iβ (residues 98-352) were built using PKA RIα (PDB: 2RGS) as a template. cGMP molecules are shown in blue. Graphs showing deuterium incorporation of selected peptides are shown, with corresponding regions colored red in the model.

Supplemental Tables

Supplemental table 1. On exchange data for PKG 4-352 –cGMP

Peptide			Exchange Time (s)						
Start	End	Charge	3	10	30	100	300	1000	3000
112	117	1	22.08%	27.48%	30.03%	36.10%	36.47%	50.94%	58.25%
112	118	1	18.54%	18.49%	25.23%	35.13%	46.49%	56.32%	67.59%
115	124	1	24.22%	28.14%	36.02%	44.67%	56.17%	69.73%	80.67%
115	124	2	29.71%	35.12%	38.86%	46.40%	55.97%	68.42%	77.08%
118	124	1	30.25%	38.17%	45.29%	50.09%	60.50%	70.14%	80.86%
118	124	2	31.03%	39.19%	44.57%	52.57%	60.85%	70.00%	80.17%
125	129	1	1.99%	2.88%	8.05%	15.55%	30.12%	51.92%	73.68%
125	132	1	3.91%	4.22%	6.23%	8.75%	14.68%	27.17%	42.69%
133	138	1	3.52%	5.22%	16.69%	25.06%	29.36%	30.21%	32.32%
136	144	1	41.61%	43.14%	52.98%	61.76%	68.28%	75.77%	82.26%
139	144	1	59.77%	62.92%	69.40%	73.72%	80.76%	92.17%	98.86%
139	145	1	38.82%	37.64%	48.06%	50.81%	57.96%	64.23%	74.49%
145	154	1	29.02%	35.87%	53.69%	70.08%	82.10%	91.80%	98.67%
145	154	2	28.91%	37.30%	52.38%	69.01%	81.65%	92.16%	98.05%
145	155	2	32.32%	38.09%	51.59%	65.47%	76.44%	87.89%	93.17%
145	156	1	22.57%	29.91%	44.63%	60.00%	68.38%	76.44%	83.05%
146	154	1	31.96%	41.77%	59.80%	77.12%	86.54%	92.93%	97.90%
146	154	2	39.87%	48.85%	60.02%	78.25%	86.20%	92.50%	97.97%
157	172	2	8.78%	15.55%	24.50%	29.32%	31.65%	34.59%	39.82%
160	172	2	10.33%	20.12%	28.56%	30.17%	31.32%	32.56%	39.35%
173	184	1	5.14%	8.57%	16.04%	23.41%	34.28%	50.11%	65.52%
173	184	2	5.82%	9.77%	15.21%	24.03%	34.93%	51.06%	65.43%
188	204	2	4.25%	9.48%	19.86%	26.25%	33.33%	40.70%	47.26%
191	204	2	4.26%	6.32%	14.39%	20.02%	25.97%	31.59%	38.57%
196	204	1	2.60%	7.80%	13.77%	19.31%	26.12%	32.93%	37.34%
196	204	2	4.15%	11.31%	14.56%	19.26%	26.03%	34.55%	40.74%
205	212	1	15.73%	24.89%	34.62%	40.77%	46.62%	52.52%	55.48%
205	212	2	15.75%	27.85%	39.53%	44.37%	49.93%	56.03%	58.87%
217	221	1	84.94%	92.73%	95.39%	101.37%	98.23%	97.42%	95.91%
217	227	1	52.80%	69.82%	93.27%	98.17%	99.68%	100.13%	100.43%
217	227	2	54.74%	72.69%	92.81%	95.81%	97.63%	98.65%	99.41%
217	230	2	38.93%	55.50%	69.68%	80.29%	90.41%	98.70%	99.82%
222	227	1	28.30%	56.28%	86.66%	97.39%	97.88%	96.76%	99.52%
222	227	2	36.75%	57.65%	81.66%	92.68%	97.43%	95.64%	94.16%
230	245	2	32.47%	33.61%	41.61%	49.31%	57.38%	68.15%	78.48%
231	243	1	37.36%	44.08%	45.72%	60.66%	67.57%	73.30%	82.18%
231	245	1	33.73%	35.26%	41.87%	49.52%	57.69%	67.12%	78.24%
231	245	2	35.46%	37.88%	42.28%	50.11%	59.41%	68.91%	78.32%
232	245	1	35.63%	38.99%	41.87%	48.39%	56.14%	65.17%	75.19%
232	245	2	34.69%	35.12%	44.44%	49.00%	56.23%	67.45%	76.52%
238	245	1	40.78%	40.08%	42.41%	45.83%	47.07%	63.41%	76.12%
241	245	1	29.22%	35.58%	35.51%	37.81%	39.31%	48.46%	64.88%

Supplemental table 1. On exchange data for PKG 4-352 –cGMP , Continued

241	248	1	37.64%	38.79%	42.79%	45.35%	53.02%	65.31%	75.49%
249	252	1	1.40%	2.33%	6.17%	6.25%	7.27%	9.57%	15.75%
251	261	1	7.62%	11.33%	16.57%	18.36%	25.75%	29.48%	35.19%
251	262	1	6.68%	11.66%	15.16%	21.85%	31.87%	38.61%	43.29%
251	262	2	5.64%	10.01%	14.87%	20.91%	28.70%	36.96%	43.08%
253	261	1	2.48%	2.84%	3.72%	6.29%	14.46%	20.11%	25.68%
253	261	2	1.66%	2.56%	2.52%	4.82%	15.19%	21.99%	27.40%
253	262	1	1.37%	2.37%	5.67%	13.26%	25.10%	33.07%	38.22%
253	262	2	1.31%	3.00%	3.54%	11.82%	23.22%	31.79%	36.53%
262	273	1	18.55%	29.38%	44.99%	55.82%	69.77%	76.79%	83.77%
262	273	2	19.91%	31.81%	45.18%	58.65%	67.94%	75.59%	79.99%
263	273	1	20.35%	32.95%	51.81%	65.97%	77.53%	85.25%	89.95%
263	273	2	24.10%	37.59%	53.86%	66.72%	78.72%	85.60%	89.46%
263	274	1	15.99%	28.52%	44.36%	59.22%	69.07%	76.66%	80.07%
263	274	2	19.84%	30.60%	46.50%	60.25%	69.93%	78.25%	81.04%
274	283	1	2.30%	2.53%	5.30%	8.78%	12.90%	14.06%	13.26%
274	295	2	13.33%	19.09%	27.43%	36.24%	43.88%	47.10%	47.72%
275	292	2	19.77%	23.33%	31.46%	36.62%	43.06%	45.71%	44.45%
296	304	2	7.24%	12.45%	21.25%	30.16%	33.77%	34.55%	36.42%
296	314	2	29.45%	41.90%	61.36%	67.76%	68.70%	69.20%	70.02%
305	314	1	50.63%	67.07%	92.16%	98.06%	98.03%	98.24%	98.58%
305	314	2	57.15%	75.44%	95.87%	99.84%	98.82%	98.07%	99.56%
305	323	2	31.63%	40.14%	55.94%	66.64%	70.64%	70.76%	72.09%
315	320	1	26.89%	31.85%	36.93%	49.36%	56.96%	58.41%	59.22%
315	320	2	28.16%	28.39%	38.16%	52.27%	55.23%	61.97%	63.19%
315	322	1	18.25%	20.62%	25.07%	31.69%	37.01%	38.23%	39.95%
315	322	2	12.16%	15.59%	25.23%	30.36%	36.43%	38.38%	39.51%
315	323	1	15.82%	18.05%	22.03%	27.71%	32.93%	34.25%	35.30%
315	324	1	13.50%	14.40%	17.85%	23.20%	27.48%	29.63%	30.85%
315	325	1	17.41%	20.17%	25.27%	31.54%	36.13%	37.70%	40.14%
315	328	1	8.65%	9.16%	16.15%	21.36%	24.33%	25.94%	25.83%
315	328	2	6.80%	8.89%	14.87%	19.38%	23.61%	24.52%	25.35%
315	329	1	6.30%	9.18%	14.77%	19.73%	22.10%	23.76%	22.92%
315	329	2	7.94%	9.60%	14.70%	18.43%	19.83%	22.46%	22.72%
315	344	3	11.75%	16.76%	24.65%	32.44%	40.32%	47.34%	52.33%
321	328	1	3.82%	9.54%	16.18%	17.05%	16.95%	18.13%	19.86%
323	329	1	4.33%	8.48%	16.83%	22.15%	21.53%	22.59%	23.79%
324	329	1	1.94%	3.09%	4.46%	5.39%	7.38%	5.98%	6.27%
325	329	1	0.89%	1.31%	0.99%	1.57%	1.50%	1.15%	1.85%
326	329	1	3.16%	2.92%	3.13%	2.31%	3.67%	3.06%	3.11%
328	343	2	17.23%	24.80%	33.93%	45.98%	60.21%	73.64%	80.37%
329	343	2	19.81%	26.70%	38.10%	49.87%	66.48%	78.44%	90.83%
329	344	1	20.39%	27.56%	39.64%	51.26%	66.30%	78.35%	90.86%
329	344	2	22.29%	28.01%	40.41%	51.48%	66.23%	77.65%	87.59%
329	352	2	45.99%	50.86%	64.61%	73.04%	81.72%	90.32%	96.20%

Supplemental table 1. On exchange data for PKG 4-352 –cGMP , Continued

329	352	3	50.02%	55.85%	64.07%	74.73%	81.54%	90.54%	95.92%
330	343	1	24.46%	29.78%	46.43%	60.24%	78.40%	92.44%	100.41%
330	343	2	22.33%	29.86%	42.41%	57.06%	71.55%	86.90%	98.50%
330	344	1	22.07%	30.13%	40.07%	55.38%	71.08%	87.01%	99.71%
330	344	2	26.43%	33.40%	45.72%	59.76%	75.32%	90.76%	96.95%
330	352	2	49.80%	55.46%	69.34%	77.60%	87.61%	95.25%	95.80%
330	352	3	51.87%	59.43%	69.60%	78.37%	86.58%	95.89%	100.56%
344	352	1	83.42%	88.09%	96.34%	97.94%	98.19%	98.95%	99.49%
345	352	1	83.82%	87.03%	96.61%	97.63%	98.11%	98.32%	99.72%

Supplemental table 2. On exchange data for PKG 4-352 +cGMP

Peptide			Exchange Time (s)						
Start	End	Charge	3	10	30	100	300	1000	3000
112	117	1	28.12%	28.97%	30.72%	34.87%	34.74%	36.95%	40.11%
112	118	1	17.42%	18.56%	20.63%	28.38%	29.38%	42.33%	44.57%
115	124	1	26.23%	30.01%	33.64%	41.62%	44.88%	53.99%	66.73%
115	124	2	26.26%	29.96%	31.85%	40.75%	48.34%	56.16%	62.79%
118	124	1	31.06%	38.13%	43.88%	50.25%	57.18%	66.63%	72.89%
118	124	2	31.91%	35.94%	39.11%	48.35%	54.04%	60.60%	69.34%
125	129	1	3.53%	5.00%	5.48%	13.12%	15.97%	30.30%	41.52%
125	132	1	3.56%	4.08%	3.38%	7.19%	8.31%	16.08%	21.65%
133	138	1	1.35%	3.33%	9.55%	16.49%	23.20%	28.05%	26.60%
136	144	1	38.65%	43.12%	46.22%	53.02%	59.68%	68.73%	73.27%
139	144	1	54.49%	55.93%	60.25%	62.77%	70.55%	87.73%	90.65%
139	145	1	37.74%	42.82%	46.29%	50.60%	50.55%	60.18%	62.71%
145	154	1	24.46%	32.56%	42.65%	56.24%	67.05%	78.59%	80.56%
145	154	2	24.92%	31.46%	41.93%	53.51%	66.76%	75.78%	81.87%
145	155	2	28.72%	32.78%	41.15%	56.27%	68.96%	76.45%	78.39%
145	156	1	22.24%	27.67%	35.88%	45.66%	56.22%	64.91%	68.94%
146	154	1	28.32%	35.84%	46.93%	62.60%	71.35%	80.13%	80.53%
146	154	2	29.77%	34.07%	48.50%	63.49%	75.04%	78.24%	82.86%
157	172	2	6.76%	13.70%	22.10%	24.52%	26.81%	28.91%	30.23%
160	172	2	7.54%	16.00%	23.81%	27.95%	27.47%	29.73%	29.62%
173	184	1	4.63%	7.94%	11.50%	14.65%	14.36%	18.42%	22.32%
173	184	2	5.94%	8.76%	10.61%	15.76%	15.54%	20.55%	23.31%
188	204	2	2.78%	6.87%	9.05%	14.61%	18.06%	22.66%	23.53%
191	204	2	2.31%	9.32%	9.62%	13.94%	16.19%	19.65%	20.70%
196	204	1	1.45%	5.41%	12.03%	18.77%	23.23%	29.43%	32.39%
196	204	2	5.20%	9.52%	13.17%	21.42%	24.41%	32.92%	32.01%
205	212	1	13.99%	22.86%	27.87%	31.02%	36.38%	42.57%	44.57%
205	212	2	15.27%	25.67%	31.18%	35.46%	40.81%	48.09%	52.04%
217	221	1	76.40%	87.77%	86.78%	85.59%	87.34%	90.85%	93.76%
217	227	1	45.61%	59.39%	70.24%	79.60%	87.58%	90.17%	90.19%
217	227	2	45.79%	64.88%	79.45%	84.07%	91.31%	91.98%	94.65%
217	230	2	32.85%	46.58%	55.37%	59.32%	70.96%	84.81%	94.95%
222	227	1	17.14%	36.64%	55.07%	75.24%	91.91%	93.55%	94.64%
222	227	2	18.77%	35.47%	54.12%	72.82%	87.59%	89.20%	93.05%
230	245	2	31.61%	33.55%	36.91%	39.69%	45.48%	51.71%	55.80%
231	243	1	33.96%	37.89%	40.59%	44.65%	53.09%	58.34%	62.85%
231	245	1	32.08%	35.06%	37.93%	40.75%	46.64%	53.24%	57.26%
231	245	2	33.69%	35.04%	38.28%	41.36%	46.93%	53.35%	57.42%
232	245	1	35.07%	36.84%	38.00%	41.25%	48.33%	56.18%	59.75%
232	245	2	35.05%	35.71%	40.12%	43.53%	50.15%	56.49%	59.03%
238	245	1	31.87%	34.62%	34.54%	36.02%	40.35%	53.71%	62.28%
241	245	1	22.73%	24.06%	24.24%	27.56%	29.04%	34.40%	40.28%
241	248	1	33.11%	34.29%	33.97%	35.37%	38.96%	52.85%	61.50%
249	252	1	1.72%	5.73%	5.73%	5.63%	5.47%	5.48%	4.91%
251	261	1	7.45%	10.05%	16.05%	19.89%	23.62%	29.64%	30.40%

Supplemental table 2. On exchange data for PKG 4-352 +cGMP, Continued

251	262	1	4.35%	10.26%	12.80%	21.41%	31.56%	36.54%	38.75%
251	262	2	4.52%	6.47%	12.66%	19.33%	30.19%	34.82%	37.75%
253	261	1	1.67%	2.75%	2.10%	7.57%	15.02%	20.75%	24.08%
253	261	2	0.91%	1.11%	-0.17%	9.56%	8.94%	16.62%	22.79%
253	262	1	1.94%	3.86%	7.12%	16.19%	25.92%	33.36%	36.05%
253	262	2	1.03%	2.14%	4.23%	13.91%	22.36%	32.22%	32.56%
262	273	1	13.35%	21.05%	31.79%	42.30%	49.28%	52.41%	56.22%
262	273	2	13.60%	21.66%	32.47%	43.64%	51.11%	53.28%	56.09%
263	273	1	14.89%	25.04%	37.76%	48.07%	56.26%	59.80%	63.46%
263	273	2	17.13%	27.02%	38.79%	49.21%	58.47%	61.23%	64.72%
263	274	1	12.63%	18.75%	32.27%	42.84%	49.54%	51.75%	55.10%
263	274	2	12.68%	21.96%	33.30%	44.61%	50.23%	53.52%	57.50%
274	283	1	-0.01%	0.77%	3.95%	7.09%	10.21%	11.11%	10.29%
274	295	2	10.27%	14.29%	15.96%	23.10%	30.14%	36.15%	37.54%
275	292	2	13.90%	21.30%	23.43%	26.04%	33.15%	35.85%	35.52%
296	304	2	4.64%	7.24%	12.53%	24.18%	28.87%	30.78%	31.38%
296	314	2	13.95%	16.89%	18.65%	24.90%	29.58%	33.11%	33.73%
305	314	1	28.03%	31.63%	33.31%	35.40%	42.57%	47.82%	49.20%
305	314	2	32.12%	34.40%	34.48%	37.27%	44.05%	46.62%	49.79%
305	323	2	15.72%	15.88%	16.12%	16.94%	19.57%	25.71%	28.03%
315	320	1	5.16%	5.36%	5.22%	6.74%	7.83%	14.48%	17.65%
315	320	2	8.22%	5.37%	5.01%	7.41%	7.92%	11.84%	17.34%
315	322	1	3.07%	3.35%	2.71%	5.01%	5.06%	9.51%	11.73%
315	322	2	4.25%	3.66%	2.76%	5.42%	4.99%	7.90%	12.14%
315	323	1	2.48%	2.75%	2.22%	3.97%	4.39%	8.09%	10.29%
315	324	1	1.91%	2.26%	2.08%	3.48%	3.43%	7.29%	9.56%
315	325	1	9.66%	9.42%	9.80%	14.68%	14.11%	17.62%	21.28%
315	328	1	2.65%	4.06%	5.56%	9.50%	8.80%	10.76%	11.85%
315	328	2	2.03%	2.93%	5.00%	8.61%	10.00%	11.06%	13.73%
315	329	1	0.07%	3.55%	3.59%	10.15%	9.65%	11.22%	11.89%
315	329	2	0.96%	2.01%	4.58%	8.23%	8.75%	9.94%	11.19%
315	344	3	6.67%	8.19%	11.77%	20.60%	25.54%	32.31%	35.83%
321	328	1	4.10%	7.67%	12.77%	16.78%	18.99%	15.24%	17.96%
323	329	1	5.01%	7.76%	15.43%	20.93%	20.21%	21.85%	20.16%
324	329	1	1.79%	2.20%	3.43%	6.56%	4.44%	3.40%	2.67%
325	329	1	3.77%	-0.55%	-0.15%	4.37%	-0.96%	1.02%	-0.94%
326	329	1	-1.89%	-0.87%	-0.86%	0.84%	6.67%	1.72%	-2.26%
328	343	2	8.94%	10.85%	17.89%	28.28%	38.81%	53.23%	55.97%
329	343	2	7.58%	11.49%	19.38%	31.09%	45.34%	57.18%	61.92%
329	344	1	11.04%	15.18%	21.36%	32.57%	45.71%	58.32%	61.67%
329	344	2	11.74%	15.13%	22.41%	33.72%	46.62%	60.57%	64.25%
329	352	2	21.53%	31.44%	43.76%	52.32%	64.24%	74.63%	75.44%
329	352	3	22.88%	33.50%	44.38%	52.36%	65.06%	73.41%	77.41%
330	343	1	14.56%	19.90%	24.56%	37.27%	51.57%	66.39%	71.03%
330	343	2	9.11%	13.20%	21.55%	36.18%	49.95%	61.54%	69.33%
330	344	1	12.90%	18.16%	22.21%	35.06%	47.75%	61.54%	66.11%
330	344	2	13.26%	18.21%	26.75%	37.89%	53.03%	65.62%	70.00%

Supplemental table 2. On exchange data for PKG 4-352 +cGMP, Continued

330	352	2	24.20%	35.79%	47.19%	55.35%	69.67%	78.61%	81.05%
330	352	3	24.31%	35.81%	47.22%	56.21%	68.89%	79.05%	81.32%
344	352	1	38.30%	59.87%	77.02%	85.39%	94.95%	96.74%	96.34%
345	352	1	42.19%	67.89%	84.66%	88.00%	91.56%	96.09%	96.05%
347	352	1	43.49%	64.98%	85.31%	91.26%	95.52%	95.85%	96.28%

Supplemental table 3. On exchange data for PKG 98-352 –cGMP

Peptide			Exchange Time (s)						
Start	End	Charge	3	10	30	100	300	1000	3000
112	117	1	10.39%	16.48%	21.21%	24.47%	27.13%	28.95%	33.50%
112	118	1	3.61%	7.39%	12.99%	15.49%	19.86%	29.85%	43.05%
115	124	1	8.26%	14.78%	19.78%	23.26%	29.53%	38.27%	49.06%
115	124	2	10.55%	16.60%	22.27%	26.27%	32.94%	42.60%	49.93%
118	124	1	10.09%	20.18%	26.67%	30.83%	35.98%	39.53%	48.40%
118	124	2	13.02%	18.28%	27.66%	30.72%	41.62%	42.50%	44.90%
125	129	1	1.53%	1.93%	2.44%	3.35%	8.75%	21.77%	40.47%
125	132	1	1.35%	2.84%	3.04%	3.37%	7.11%	13.42%	25.64%
133	138	1	1.27%	2.78%	2.76%	2.45%	10.53%	24.52%	31.76%
136	144	1	24.84%	36.65%	45.81%	52.71%	57.86%	65.45%	74.93%
139	144	1	41.20%	54.87%	67.51%	68.51%	72.17%	76.12%	87.54%
139	145	1	33.75%	42.82%	47.77%	49.81%	53.29%	57.01%	63.41%
145	154	1	18.82%	26.85%	35.20%	48.52%	70.26%	85.64%	96.02%
145	154	2	19.12%	27.35%	33.11%	48.60%	70.46%	89.01%	95.22%
145	155	2	15.49%	25.19%	32.27%	44.09%	65.67%	78.71%	90.28%
145	156	1	16.55%	24.35%	31.14%	40.28%	56.70%	70.21%	77.92%
146	154	1	21.51%	30.72%	39.07%	52.01%	73.57%	89.68%	94.98%
146	154	2	20.50%	31.72%	39.44%	53.12%	76.85%	91.31%	95.34%
157	172	2	2.95%	4.13%	7.61%	14.80%	22.01%	29.01%	34.56%
160	172	2	2.33%	4.46%	9.64%	17.00%	27.34%	30.63%	34.86%
173	184	1	3.02%	4.07%	6.76%	14.69%	29.03%	44.42%	56.94%
173	184	2	3.41%	3.55%	8.11%	14.74%	29.05%	44.73%	58.89%
188	204	2	4.87%	7.81%	12.40%	18.76%	26.07%	32.59%	40.54%
191	204	2	3.54%	6.34%	7.67%	11.71%	17.37%	22.46%	31.08%
196	204	1	0.95%	1.82%	3.87%	8.21%	14.61%	19.78%	28.82%
196	204	2	0.22%	0.34%	3.07%	6.99%	14.81%	20.29%	29.89%
205	212	1	8.85%	14.99%	26.42%	37.04%	43.53%	47.33%	52.80%
205	212	2	7.99%	15.78%	28.49%	39.87%	46.33%	50.77%	53.11%
217	221	1	27.74%	54.97%	82.41%	96.88%	97.65%	98.10%	99.53%
217	227	1	15.04%	33.68%	57.44%	76.25%	92.63%	99.73%	100.26%
217	227	2	15.14%	34.50%	57.49%	76.49%	92.67%	97.38%	99.23%
217	230	2	12.08%	23.03%	40.74%	58.53%	71.38%	82.48%	92.91%
222	227	1	8.44%	17.18%	36.46%	52.06%	74.69%	87.08%	92.44%
222	227	2	9.97%	17.49%	35.38%	54.08%	71.15%	92.66%	94.70%
230	245	2	21.90%	30.67%	34.27%	35.42%	39.03%	45.90%	54.77%
231	243	1	29.06%	38.79%	42.15%	45.80%	50.33%	59.26%	69.79%
231	245	1	23.11%	33.03%	36.96%	38.27%	41.53%	48.69%	57.32%
231	245	2	23.67%	32.72%	37.06%	38.02%	41.37%	48.81%	57.07%
232	245	1	26.02%	36.91%	40.66%	42.46%	44.23%	48.68%	56.02%
232	245	2	25.98%	34.78%	39.24%	39.60%	44.15%	48.99%	55.62%
238	245	1	18.52%	33.77%	40.99%	41.05%	42.18%	44.92%	50.93%
241	245	1	18.01%	29.81%	36.06%	37.76%	38.88%	40.01%	44.49%
241	248	1	17.94%	33.53%	41.30%	41.03%	41.92%	43.81%	50.66%

Supplemental table 3. On exchange data for PKG 98-352 –cGMP, Continued

249	252	1	1.51%	1.84%	2.97%	2.69%	3.63%	3.91%	4.19%
251	261	1	2.60%	6.83%	10.46%	15.94%	18.20%	20.65%	28.06%
251	262	1	3.40%	6.04%	9.88%	14.79%	18.52%	25.43%	34.10%
251	262	2	3.50%	5.52%	8.97%	14.05%	17.09%	24.50%	33.50%
253	261	1	2.09%	2.12%	3.13%	3.51%	5.53%	9.58%	16.79%
253	261	2	4.21%	4.57%	4.53%	4.79%	6.67%	10.77%	18.72%
253	262	1	1.98%	1.78%	2.26%	3.54%	6.51%	13.89%	25.87%
253	262	2	2.34%	2.60%	2.77%	4.17%	8.03%	13.34%	27.80%
262	273	1	9.58%	12.89%	18.50%	28.41%	43.18%	56.77%	67.57%
262	273	2	8.66%	13.02%	19.35%	30.06%	45.48%	56.92%	69.73%
263	273	1	10.84%	15.20%	22.29%	35.20%	51.41%	66.01%	77.48%
263	273	2	13.05%	16.45%	24.18%	36.36%	52.51%	66.97%	76.92%
263	274	1	7.76%	10.84%	17.42%	28.66%	42.93%	55.77%	65.70%
263	274	2	8.20%	11.65%	18.86%	30.89%	44.94%	58.25%	67.75%
274	283	1	1.10%	1.83%	2.20%	2.28%	4.38%	7.47%	11.35%
274	295	2	4.79%	7.65%	11.79%	17.03%	24.56%	33.07%	41.49%
275	292	2	8.22%	12.40%	18.55%	24.37%	30.21%	36.89%	44.88%
296	304	2	4.17%	5.15%	6.61%	9.38%	20.92%	28.82%	32.85%
296	314	2	14.76%	23.99%	33.99%	44.78%	59.56%	67.87%	69.55%
305	314	1	23.24%	38.80%	52.75%	66.26%	85.92%	95.28%	96.09%
305	314	2	24.97%	40.39%	53.90%	67.41%	87.15%	97.95%	98.78%
305	323	2	15.89%	23.32%	31.31%	37.04%	51.46%	65.39%	71.25%
315	320	1	25.17%	29.32%	30.11%	32.31%	35.24%	44.60%	55.90%
315	320	2	24.27%	29.95%	30.61%	30.33%	36.02%	44.97%	53.87%
315	322	1	16.73%	18.34%	19.23%	20.04%	23.18%	29.00%	35.89%
315	322	2	16.28%	18.86%	19.32%	21.45%	22.49%	31.23%	34.28%
315	323	1	14.52%	16.75%	17.11%	17.62%	20.65%	26.26%	31.75%
315	324	1	12.55%	13.88%	14.50%	15.28%	17.34%	21.88%	27.52%
315	325	1	12.04%	14.21%	14.78%	18.12%	23.29%	31.55%	35.97%
315	328	1	6.13%	8.06%	9.59%	11.28%	14.82%	21.16%	23.07%
315	328	2	7.21%	7.98%	8.82%	11.66%	16.10%	21.12%	24.03%
315	329	1	5.76%	5.82%	6.81%	9.40%	14.27%	17.75%	21.94%
315	329	2	5.96%	6.67%	7.34%	8.94%	11.97%	16.45%	19.15%
315	344	3	6.63%	9.75%	13.95%	17.45%	23.83%	31.33%	39.61%
321	328	1	1.33%	2.58%	2.94%	7.67%	11.04%	14.96%	17.43%
323	329	1	1.83%	2.36%	4.13%	8.45%	16.94%	19.02%	19.45%
324	329	1	2.76%	3.23%	2.72%	4.82%	6.24%	7.13%	7.00%
325	329	1	0.92%	2.07%	3.59%	3.62%	2.38%	3.80%	3.12%
326	329	1	0.97%	1.46%	2.04%	3.40%	5.21%	6.02%	8.17%
328	343	2	9.22%	13.96%	20.34%	25.56%	34.26%	45.45%	58.74%
329	343	2	9.30%	15.84%	22.31%	28.43%	37.29%	49.39%	65.20%
329	344	1	10.38%	16.28%	24.14%	30.88%	39.28%	51.99%	66.73%
329	344	2	11.28%	18.04%	25.54%	31.49%	41.26%	54.08%	68.29%
329	352	2	24.97%	40.32%	51.17%	57.33%	65.71%	74.09%	82.94%
329	352	3	25.01%	40.20%	50.04%	51.89%	60.15%	72.16%	80.68%
330	343	1	11.92%	18.71%	26.99%	34.40%	42.51%	58.15%	76.76%
330	343	2	11.44%	17.33%	25.90%	32.73%	43.18%	58.45%	73.71%

Supplemental table 3. On exchange data for PKG 98-352 –cGMP, Continued

330	344	1	12.58%	18.39%	28.91%	34.29%	45.19%	58.40%	75.41%
330	344	2	11.84%	21.70%	29.98%	36.16%	45.22%	60.80%	76.33%
330	352	2	27.45%	44.77%	56.05%	61.87%	70.49%	79.51%	88.83%
330	352	3	28.69%	45.30%	57.13%	62.45%	70.50%	80.17%	89.93%
344	352	1	46.58%	71.40%	87.54%	92.31%	97.73%	97.81%	97.98%
345	352	1	53.27%	75.23%	88.28%	89.54%	92.82%	96.97%	97.73%
347	352	1	43.44%	75.45%	83.99%	89.89%	94.54%	97.06%	98.15%

Supplemental table 4. On exchange data for PKG 98-352 +cGMP

Peptide			Exchange Time (s)						
Start	End	Charge	3	10	30	100	300	1000	3000
112	117	1	10.19%	18.38%	25.65%	26.18%	26.46%	28.28%	28.84%
112	118	1	5.25%	8.32%	12.01%	15.07%	15.99%	21.65%	35.89%
115	124	1	7.75%	17.03%	22.59%	26.25%	30.12%	35.68%	48.50%
115	124	2	10.20%	17.36%	24.60%	29.36%	33.03%	42.25%	53.21%
118	124	1	11.78%	22.33%	31.07%	37.84%	42.11%	46.01%	52.57%
118	124	2	12.66%	29.12%	36.85%	38.77%	42.84%	43.89%	57.37%
125	129	1	1.87%	2.38%	1.87%	1.71%	2.41%	3.67%	6.45%
125	132	1	3.18%	3.48%	3.57%	3.84%	4.70%	5.32%	5.69%
133	138	1	1.07%	1.66%	1.85%	5.80%	10.51%	23.62%	32.66%
136	144	1	25.08%	34.47%	44.71%	50.95%	57.26%	64.56%	71.22%
139	144	1	39.28%	55.32%	66.21%	66.51%	71.32%	74.27%	80.61%
139	145	1	32.83%	38.78%	46.87%	49.35%	51.85%	54.06%	60.12%
145	154	1	20.01%	26.12%	31.00%	37.41%	51.15%	65.31%	75.59%
145	154	2	20.96%	25.23%	29.50%	34.56%	52.38%	65.64%	78.94%
145	155	2	18.52%	27.94%	31.08%	37.81%	44.78%	61.33%	71.10%
145	156	1	18.00%	24.91%	28.08%	32.56%	44.32%	55.38%	61.96%
146	154	1	22.91%	28.18%	34.10%	40.71%	54.67%	69.54%	77.77%
146	154	2	24.76%	31.46%	35.24%	43.25%	55.65%	68.31%	78.30%
157	172	2	2.40%	3.72%	7.57%	14.78%	23.28%	25.98%	28.62%
160	172	2	2.49%	4.42%	9.19%	16.64%	25.48%	29.96%	30.31%
173	184	1	1.77%	2.50%	4.40%	7.69%	12.50%	13.45%	13.65%
173	184	2	1.35%	1.98%	4.62%	7.86%	12.18%	13.18%	14.47%
188	204	2	0.91%	2.48%	4.17%	8.17%	14.21%	17.25%	20.05%
191	204	2	1.39%	1.65%	2.82%	5.39%	9.65%	12.28%	17.15%
196	204	1	1.04%	2.36%	3.30%	6.11%	13.84%	19.46%	24.81%
196	204	2	0.61%	0.62%	2.42%	7.94%	14.52%	19.19%	23.73%
205	212	1	5.79%	11.90%	23.18%	31.91%	35.22%	36.24%	41.19%
205	212	2	6.43%	14.23%	25.95%	32.71%	38.39%	40.63%	46.39%
217	221	1	37.48%	66.32%	91.23%	98.18%	99.23%	98.05%	98.90%
217	227	1	16.98%	34.80%	58.31%	77.19%	88.04%	94.87%	99.85%
217	227	2	16.49%	34.49%	57.84%	75.18%	86.62%	95.69%	98.55%
217	230	2	12.06%	24.82%	41.95%	57.70%	64.96%	73.00%	79.23%
222	227	1	3.81%	10.62%	24.14%	40.34%	59.98%	79.82%	91.65%
222	227	2	3.41%	13.04%	29.98%	45.32%	63.06%	80.69%	90.29%
230	245	2	19.13%	28.11%	33.78%	34.92%	36.79%	40.21%	44.14%
231	243	1	26.06%	35.77%	42.85%	44.88%	47.40%	52.38%	56.36%
231	245	1	21.23%	30.38%	36.49%	37.90%	40.26%	44.16%	48.86%
231	245	2	20.55%	30.52%	35.63%	38.00%	40.01%	42.06%	47.82%
232	245	1	22.58%	33.01%	39.98%	41.72%	43.74%	49.42%	53.82%
232	245	2	22.51%	32.08%	39.56%	40.85%	43.11%	47.32%	51.76%
238	245	1	16.84%	30.88%	38.47%	40.09%	42.41%	43.05%	44.22%
241	245	1	13.36%	27.77%	36.54%	37.12%	38.92%	40.65%	41.88%
241	248	1	16.88%	30.76%	38.30%	39.96%	41.18%	42.85%	44.15%

Supplemental table 4. On exchange data for PKG 98-352 +cGMP, Continued

249	252	1	2.63%	2.12%	3.75%	5.09%	4.76%	4.25%	6.04%
251	261	1	3.00%	4.54%	9.15%	13.71%	17.62%	19.43%	26.14%
251	262	1	2.76%	4.37%	8.36%	14.02%	20.98%	27.79%	37.59%
251	262	2	2.19%	4.94%	6.76%	12.37%	18.76%	26.39%	34.69%
253	261	1	2.87%	2.72%	3.04%	4.07%	5.31%	9.26%	16.79%
253	261	2	3.02%	3.61%	4.73%	5.94%	7.78%	9.17%	16.98%
253	262	1	2.36%	2.66%	2.79%	4.35%	9.14%	16.63%	29.13%
253	262	2	1.31%	1.08%	2.83%	4.66%	9.34%	15.08%	30.26%
262	273	1	9.77%	10.22%	14.73%	22.91%	36.36%	46.33%	51.31%
262	273	2	10.14%	11.25%	16.71%	23.88%	37.95%	47.43%	52.82%
263	273	1	11.51%	12.82%	18.07%	27.66%	43.12%	54.33%	59.53%
263	273	2	13.27%	13.91%	19.56%	29.51%	44.08%	54.54%	59.85%
263	274	1	7.62%	9.63%	13.88%	21.79%	34.97%	44.93%	50.17%
263	274	2	8.41%	9.95%	14.10%	23.59%	36.68%	47.90%	50.96%
274	283	1	1.08%	1.23%	1.55%	1.80%	4.67%	8.66%	12.57%
274	295	2	4.74%	6.88%	9.84%	13.80%	19.42%	24.32%	29.85%
275	292	2	6.59%	10.76%	16.73%	22.98%	27.62%	29.54%	35.94%
296	304	2	2.94%	3.25%	4.51%	7.45%	12.10%	23.83%	31.81%
296	314	2	11.30%	14.03%	17.83%	19.18%	22.90%	27.34%	32.96%
305	314	1	18.38%	26.41%	32.64%	37.01%	38.62%	40.38%	46.06%
305	314	2	19.41%	27.01%	34.95%	37.35%	39.03%	42.20%	49.26%
305	323	2	8.26%	12.10%	13.85%	14.82%	16.00%	18.66%	21.03%
315	320	1	4.48%	4.96%	5.86%	6.03%	7.25%	8.04%	13.21%
315	320	2	4.70%	6.62%	8.53%	8.91%	10.15%	10.74%	17.02%
315	322	1	3.02%	3.30%	3.53%	3.62%	4.36%	5.19%	8.30%
315	322	2	3.24%	3.32%	4.12%	4.20%	5.39%	5.61%	10.18%
315	323	1	2.62%	3.15%	3.51%	3.58%	4.11%	5.20%	7.59%
315	324	1	2.28%	2.38%	2.59%	2.53%	3.00%	3.74%	6.09%
315	325	1	3.97%	4.41%	5.88%	7.65%	12.72%	16.20%	16.96%
315	328	1	-0.46%	1.13%	1.90%	3.39%	7.26%	10.99%	11.77%
315	328	2	1.39%	1.33%	1.99%	4.66%	7.78%	10.12%	12.02%
315	329	1	-0.23%	0.72%	1.22%	3.37%	6.63%	6.92%	10.83%
315	329	2	0.38%	0.82%	1.90%	3.28%	6.20%	7.98%	8.94%
315	344	3	3.70%	4.87%	6.81%	9.89%	16.82%	23.09%	28.04%
321	328	1	-0.08%	1.93%	2.87%	5.12%	12.93%	15.50%	17.58%
323	329	1	1.48%	2.23%	2.82%	7.66%	17.09%	19.94%	21.45%
324	329	1	2.45%	2.43%	2.55%	2.71%	3.88%	3.72%	4.92%
325	329	1	1.72%	2.20%	2.56%	3.09%	3.48%	3.13%	3.26%
326	329	1	-0.09%	2.17%	3.60%	2.82%	2.63%	3.65%	5.67%
328	343	2	4.27%	6.03%	9.58%	14.75%	23.13%	35.16%	46.79%
329	343	2	4.61%	6.46%	11.09%	16.49%	28.09%	39.47%	51.62%
329	344	1	7.79%	10.40%	14.44%	19.69%	30.07%	41.91%	53.57%
329	344	2	8.00%	11.21%	15.20%	20.91%	31.65%	43.35%	55.62%
329	352	2	8.86%	15.15%	24.25%	36.02%	50.62%	62.71%	73.77%
329	352	3	8.78%	16.38%	23.93%	35.47%	49.02%	60.64%	70.13%
330	343	1	6.07%	8.32%	13.30%	19.45%	33.33%	46.88%	61.32%
330	343	2	5.08%	7.96%	12.99%	19.86%	30.87%	47.34%	59.19%

Supplemental table 4. On exchange data for PKG 98-352 +cGMP, Continued

330	344	1	9.08%	12.54%	17.46%	23.01%	35.28%	48.27%	60.53%
330	344	2	10.45%	12.80%	17.90%	24.31%	36.31%	48.97%	62.96%
330	352	2	10.40%	16.39%	27.20%	39.92%	55.31%	68.70%	78.65%
330	352	3	10.41%	17.07%	26.17%	38.88%	55.21%	67.26%	78.42%
344	352	1	9.64%	19.59%	37.70%	58.62%	79.27%	91.20%	96.45%
345	352	1	13.44%	25.22%	46.49%	66.23%	87.45%	99.45%	99.68%
347	352	1	10.45%	21.19%	41.90%	63.10%	84.45%	96.12%	97.98%

References

1. Engen, J. R. and Smith, D. L. Anal. Chem. 2001, 73, 256A– 265A.

2. Englander, S. W., Mayne, L., Bai, Y., and Sosnick, T. R. Hydrogen exchange: the modern legacy of Linderstrom-Lang. Protein Sci, 6: 1101-1109, 1997.

3. Woods, V. L., Jr. and Hamuro, Y. High resolution, high-throughput amide deuterium exchange-mass spectrometry (DXMS) determination of protein binding site structure and dynamics: utility in pharmaceutical design. J Cell Biochem Suppl, Suppl 37: 89-98, 2001.

4. Engen, John R. Analysis of Protein Conformation and Dynamics by Hydrogen/Deuterium Exchange MS. Anal. Chem, 81: 7870-7875, 2009.

5. Wales, T. E. and Engen, J. R. Mass Spectrom. Rev. 2006, 25, 158– 170

6. Dyson HJ, Wright PE. 2004. Unfolded proteins and protein folding studied by NMR. Chem Rev 104: 3607-3622

7. Hamuro, Y., Coales, S. J., Southern, M. R., Nemeth-Cawley, J. F., Stranz, D. D., and Griffin, P. R. Rapid analysis of protein structure and dynamics by hydrogen/deuterium exchange mass spectrometry. J Biomol Tech, 14: 171-182, 2003.

8. Tsutsui Y, Wintrode PL. Hydrogen/deuterium exchange-mass spectrometry: a powerful tool for probing protein structure, dynamics and interactions. Curr. Med. Chem. 2007;14:2344-2358.

9. R. S. Molday, S. W. Englander, R. G. Kallen. Primary structure effects on peptide group hydrogen exchange. Biochemistry,11 (2), pp 150–158, 1972.

10. Englander SW, Mayne L, Bai Y, Sosnick TR. Hyd Hydrogen exchange: the modern legacy of Linderstrøm-Lang. Protein Science. 1997;6:1101-1109.

11. Laura S. Busenlehner and Richard N. Armstrong. Insights into enzyme structure and dynamics elucidated by amide H/D exchange mass spectrometry. Biochemistry and Biophysics, Volume 433, Issue 1: 34-46, 2005.

12. Feil, R., Hofmann, F. & Kleppisch, T. (2005) Rev Neurosci 16, 23-41.

13. Hofmann, F., Bernhard, D., Lukowski, R. & Weinmeister, P. (2009) Handb Exp Pharmacol, 137-62.

14. Ruth, P., Pfeifer, A., Kamm, S., Klatt, P., Dostmann, W. R. & Hofmann, F. (1997) J Biol Chem 272, 10522-8.

15. Richie-Jannetta, R., Francis, S. H. & Corbin, J. D. (2003) J Biol Chem 278, 50070-9.

16. Casteel, D. E., Zhuang, S., Gudi, T., Tang, J., Vuica, M., Desiderio, S. & Pilz, R. B. (2002) J Biol Chem 277, 32003-14.

17. Yuasa, K., Michibata, H., Omori, K. & Yanaka, N. (1999) J Biol Chem 274, 37429-34.

18. Yuasa, K., Omori, K. & Yanaka, N. (2000) J Biol Chem 275, 4897-905.

19. Surks, H. K., Mochizuki, N., Kasai, Y., Georgescu, S. P., Tang, K. M., Ito, M., Lincoln, T. M. & Mendelsohn, M. E. (1999) Science 286, 1583-7.

20. Tang, K. M., Wang, G. R., Lu, P., Karas, R. H., Aronovitz, M., Heximer, S. P., Kaltenbronn, K. M., Blumer, K. J., Siderovski, D. P., Zhu, Y. & Mendelsohn, M. E. (2003) Nat Med 9, 1506-12.

21. Ammendola, A., Geiselhoringer, A., Hofmann, F. & Schlossmann, J. (2001) J Biol Chem 276, 24153-9.

22. Casteel, D. E., Boss, G. R. & Pilz, R. B. (2005) J Biol Chem 280, 38211-8.

23. Richie-Jannetta, R., Busch, J. L., Higgins, K. A., Corbin, J. D. & Francis, S. H. (2006) J Biol Chem 281, 6977-84.

24. Busch, J. L., Bessay, E. P., Francis, S. H. & Corbin, J. D. (2002) J Biol Chem 277, 34048-54.

25. Wolfe, L., Francis, S. H. & Corbin, J. D. (1989) J Biol Chem 264, 4157-62.

26. Woods, V. L., Jr. & Hamuro, Y. (2001) J Cell Biochem Suppl Suppl 37, 89-98.

27. Alverdi, V., Mazon, H., Versluis, C., Hemrika, W., Esposito, G., van den Heuvel, R., Scholten, A. & Heck, A. J. (2008) J Mol Biol 375, 1380-93.

28 Hamuro, Y., Anand, G. S., Kim, J. S., Juliano, C., Stranz, D. D., Taylor, S. S. & Woods, V. L., Jr. (2004) J Mol Biol 340, 1185-96.

29. Burns-Hamuro, L. L., Hamuro, Y., Kim, J. S., Sigala, P., Fayos, R., Stranz, D. D., Jennings, P. A., Taylor, S. S. & Woods, V. L., Jr. (2005) *Protein Sci* **14,** 2982-92.

30. Pantazatos, D., Kim, J. S., Klock, H. E., Stevens, R. C., Wilson, I. A., Lesley, S. A. Woods, V. L., Jr. (2004) *Proc Natl Acad Sci U S A* **101,** 751-6.

31. Zhang, Z. and Smith, D. L. (1993) Protein Sci. 2, 522– 531.

32. Reed, R. B., Sandberg, M., Jahnsen, T., Lohmann, S. M., Francis, S. H. & Corbin, J. D. (1996) J Biol Chem 271, 17570-5.

33. Francis, S. H. & Corbin, J. D. (1999) Crit Rev Clin Lab Sci 36, 275-328.

34. Feil, R., Bigl, M., Ruth, P. & Hofmann, F. (1993) Mol Cell Biochem 127-128, 71-80.

35. Dostmann, W. R., Koep, N. & Endres, R. (1996) FEBS Lett 398, 206-10.

36. Su, Y., Dostmann, W. R., Herberg, F. W., Durick, K., Xuong, N. H., Ten Eyck, L., Taylor, S. S. & Varughese, K. I. (1995) Science 269, 807-13.

37. Diller, T. C., Madhusudan, Xuong, N. H. & Taylor, S. S. (2001) Structure 9, 73-82.

38. Kim, C., Cheng, C. Y., Saldanha, S. A. & Taylor, S. S. (2007) Cell 130, 1032-43.

39. Kornev, A. P., Taylor, S. S. & Ten Eyck, L. F. (2008) PLoS Comput Biol 4, e1000056.

40. Brown, S. H., Wu, J., Kim, C., Alberto, K. & Taylor, S. S. (2009) J Mol Biol 393, 1070-82.

41. Vigil, D., Blumenthal, D. K., Brown, S., Taylor, S. S. & Trewhella, J. (2004) Biochemistry 43, 5629-36.

42. Smith, J. A., Francis, S. H., Walsh, K. A., Kumar, S. & Corbin, J. D. (1996) J Biol Chem 271, 20756-62.

43. Hamuro, Y., Anand, G. S., Kim, J. S., Juliano, C., Stranz, D. D., Taylor, S. S. & Woods, V. L., Jr. (2004) J Mol Biol 340, 1185-96.

44. Hamuro, Y., Zawadzki, K. M., Kim, J. S., Stranz, D. D., Taylor, S. S. & Woods, V. L., Jr. (2003) J Mol Biol 327, 1065-76.

45. Kern, D. & Zuiderweg, E. R. (2003) Curr Opin Struct Biol 13, 748-57.

46. Huang, Y. J. & Montelione, G. T. (2005) Nature 438, 36-7.

47. Kinderman, F. S., Kim, C., von Daake, S., Ma, Y., Pham, B. Q., Spraggon, G., Xuong, N. H., Jennings, P. A. & Taylor, S. S. (2006) Mol Cell 24, 397-408.

48. Sarma, G. N., Kinderman, F. S., Kim, C., von Daake, S., Chen, L., Wang, B. C. & Taylor, S. S. Structure 18, 155-66.

49. Gold, M. G., Lygren, B., Dokurno, P., Hoshi, N., McConnachie, G., Tasken, K., Carlson, C. R., Scott, J. D. & Barford, D. (2006) Mol Cell 24, 383-95.

50. Trewhella, J. (2006) Eur Biophys J 35, 585-9.